

The Impacts of Multiscale Weather Systems on Freezing Rain and Snowstorms over Southern China

JIANHUA SUN AND SIXIONG ZHAO

Institute of Atmospheric Physics, Chinese Academy of Sciences, Beijing, China

(Manuscript received 18 December 2008, in final form 14 July 2009)

ABSTRACT

This paper investigated the interactions between the synoptic patterns, quasi-stationary fronts, eastward-propagating cloud clusters from the Tibetan Plateau, surface conditions, and atmospheric stratification processes associated with a 20-day event of freezing precipitation over southern China from January to February 2008. It was found that the long duration of the freezing precipitation process was primarily caused by stationary and anomalous synoptic weather patterns such as a blocking high pressure system in the northern branch and a trough in the south branch of the westerlies, which resulted in the convergence of cold air from northern China and warm, moist air from the south. The cloud clusters over the Tibetan Plateau propagated eastward and showed noticeable impacts in the local areas when they moved over southern China during several similar cloud propagation processes from January to February 2008. An east–west-oriented quasi-stationary front system in southern China, which is rare during the Asian winter monsoon season, is responsible for producing freezing precipitation and snowstorms. A stronger horizontal gradient of the isolines of the pseudo-equivalent potential temperature and higher temperatures at the inversion layer in the western part of the front than that in its eastern part can be found. At the same time, low-level moisture convergence ahead of the front enhanced the formation, development, and persistence of freezing precipitation in the west part of the front. The thickness of the warm layer and the temperature inversion layer also modulated the intensity and duration of freezing rain and ice pellets. Temperature from about -1° to -3°C and weak winds were found to be favorable meteorological factors at the surface level for freezing precipitation. These analysis results are synthesized into a conceptual model that coherently describes the physics processes associated with the synoptic features and quasi-stationary front system as well as the atmospheric stratification process during the freezing precipitation event.

1. Introduction

Freezing precipitation, including freezing drizzle (FZDZ), freezing rain (FZRA), and ice pellets (IPE; Carrière et al. 2000; Bernstein 2000), is a major weather hazard that can cause severe socioeconomic losses. Surface ice accumulation can halt air and ground transportation, weigh down and snap power lines, severely damage trees, and it is also a potential serious risk to the safety and health of local residents in the influenced areas. Four stages of heavy snowfall and freezing precipitation were observed almost continuously over southern China from January to February 2008: 0000 UTC 11 January–0000 UTC 17 January (stage I), 0000 UTC

18 January–0000 UTC 22 January (stage II), 0000 UTC 25 January–0000 UTC 30 January (stage III), and 0000 UTC 31 January–0000 UTC 2 February (stage IV), respectively. From 11 January to 2 February 2008, the intensive snowfall and freezing precipitation resulted in the most severe damage to the local transportation, electric power lines, communication systems, agriculture, and forestry since 1950, especially during stages II and III (cases are shown in Fig. 1). The most severe damage was found between 25° and 30°N , in the areas of Hunan, Guizhou, and Jiangxi Provinces (Fig. 2), where the persistent FZRA occurred. The ice on power lines was more than 60 mm thick (Zhao et al. 2008), which consequently led to the collapse of several electricity transmission towers (Fig. 1). Frozen highways in Guangdong and Hunan Provinces were closed for several weeks. Hundreds of thousands of people who were traveling for the Chinese New Year (spring festival) had to spend days or even weeks in railway stations. Crops

Corresponding author address: Dr. Jianhua Sun, Institute of Atmospheric Physics, Chinese Academy of Sciences, P.O. Box 9804, Beijing 100029, China.
E-mail: sjh@mail.iap.ac.cn

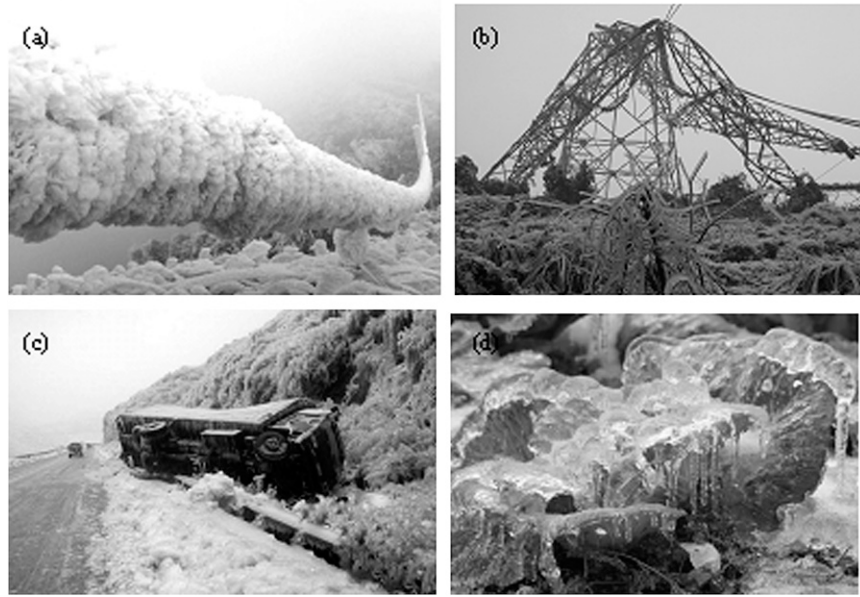


FIG. 1. Examples of the disastrous impacts of freezing rain in southern China from January to February 2008: (a) frozen electrical wires, (b) a collapsed electricity tower, (c) a frozen road and an overturning car, and (d) frozen vegetations and crops (obtained online at <http://www.sina.com.cn> and the Xinhua Web site).

on 178 millions acres were severely damaged. During the 20 days of this freezing precipitation event, 129 people died and the total economic loss was estimated to be about 151.65 billion Chinese yuan ($\sim \$21$ billion U.S.).

Given the huge impacts of FZRA, many studies have been conducted to investigate them and to try and understand the synoptic background and weather conditions for freezing precipitation events. The previous studies have mainly focused on various regions in North America and Europe, while only very limited number of studies were conducted in China. The investigations in the past with respect to the prediction of freezing precipitation or precipitation types generally fall into the following three categories:

- (a) Statistical models [e.g., critical thresholds, regression analysis, model output statistics (MOS), cluster diagnosis of synoptic weather types or patterns] were developed for improving the short-term forecasts of FZRA. Czys et al. (1996) derived a nondimensional parameter (relevant to the residence time of the ice particles) to enhance the diagnosis of conditions favorable for the occurrence of FZRA and IPE. Bocchieri (1980) used the regression method on radiosonde observations to estimate the occurrence probability in order to diagnose winter precipitation type.
- (b) Climatological analyses were conducted for characterizing the weather conditions most favorable for freezing precipitation (Carrière et al. 2000; Changnon and Karl 2003; Cortinas et al. 2004; Houston and Changnon 2007). Houston and Changnon (2007) studied U.S. FZRA from 1928 to 2001 and indicated that most FZRA occurrences were at areas with dry-bulb temperatures of -2.2° to 0°C and dewpoint temperatures of -2.8° to -0.6°C . They also found that hourly precipitation amounts during FZRA were light (usually less than 2.5 mm) and wind speeds during FZRA were typically weak and from the northeast quadrant. High wind speeds with relatively high precipitation amounts were not common conditions during FZRA. Cortinas et al. (2004) revealed that the occurrences of FZRA and FZDZ in the United States and Canada were most often during periods just before sunrise and the least frequent were near sunset, and the most favorable temperature conditions were when the surface (2 m) temperature was slightly below 0°C . In Europe, Carrière et al. (2000) found that freezing precipitation is most frequent during December–February and more frequent in Germany and central Europe, and that the dominant types are FZRA and FZDZ (as opposed to IPE).
- (c) Composite analyses of individual FZRA events were carried out to reveal the physical mechanisms of freezing precipitation (Bernstein 2000; Coleman and Marwitz 2002; Forbes et al. 1987; Rauber et al. 1994, 2000; Stewart 1985; Stewart and King 1987).

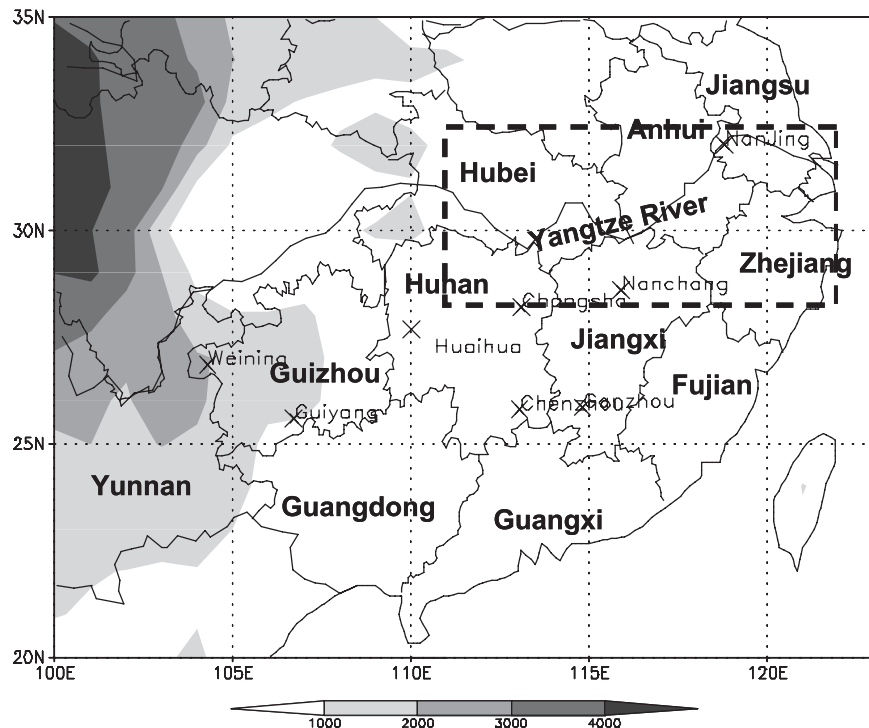


FIG. 2. The distribution of district and upper-air radiosonde stations over southern China, including the following eight soundings: Weining, Guiyang, Huaihua, Changsha, Chenzhou, Ganzhou, Nanchang, and Nanjing. The rectangle shows the middle and lower reaches of the Yangtze River. The shading represents terrain higher than 1000 m.

A good understanding of the processes producing freezing precipitation requires a thorough knowledge of the meteorological conditions at the surface and upper levels of the atmosphere. Rauber et al. (1994) reported a severe 20-h FZRA event over the midwestern United States from 14 to 15 February 1990 that occurred to the north of a slow-moving warm front.

The past studies of the previously mentioned three categories have firmly established the two microphysical mechanisms, namely, collision-coalescence (warm rain) and melting processes, as the major processes for freezing precipitation development (Bocchieri 1980; Huffman and Norman 1988). The warm-rain processes typically occur in situations where clouds are primarily composed of liquid water near freezing temperatures and cloud-top temperatures are typically greater than -10°C (to suppress the large production of snow; Rauber et al. 2000). A melting layer is needed to melt the snow; the melted snow then falls in the subfreezing layer to form supercooled rain. However, Carrière et al. (2000) indicated that the most frequent mechanisms for the formation of freezing precipitation seem to be the ice processes, with the existence of a warm layer ($>0^{\circ}\text{C}$) where ice crystals

melt, although about 30%–40% of the cases of FZRA and FZDZ that show no warm layers in the clouds.

Ding and Krishnamurti (1987) studied cold-air outbreaks and their associated significant weather events over China, Korea, and Japan, including strong cold fronts, high winds, abrupt temperature drops, and intense cyclones. To date, there is little knowledge about freezing precipitation associated with moderately intensive fronts and weak wind conditions during Asian winter monsoon season. In China, freezing precipitation occurs most frequently over Guizhou Province, followed by the regions of Hunan, Jiangxi, Hubei, Henan, Anhui, and Jiangsu Provinces (cited from the China Meteorological Agency Web site: <http://www.cma.gov.cn>). Generally, freezing precipitation occurs more frequently over mountainous areas than over the plains in China, and one typical example is in the area of Guizhou Province (Ye et al. 2007). Moreover, research efforts in China into winter freezing precipitation are much less common than are studies of summer heavy rainfall. Only a few weather forecasters have experience with predicting freezing precipitation (Chen et al. 1993; Yang 1999; Lv et al. 2004). Their results indicated that favorable conditions for freezing precipitation are stable stratification, an inversion, and a near 0°C surface temperature.

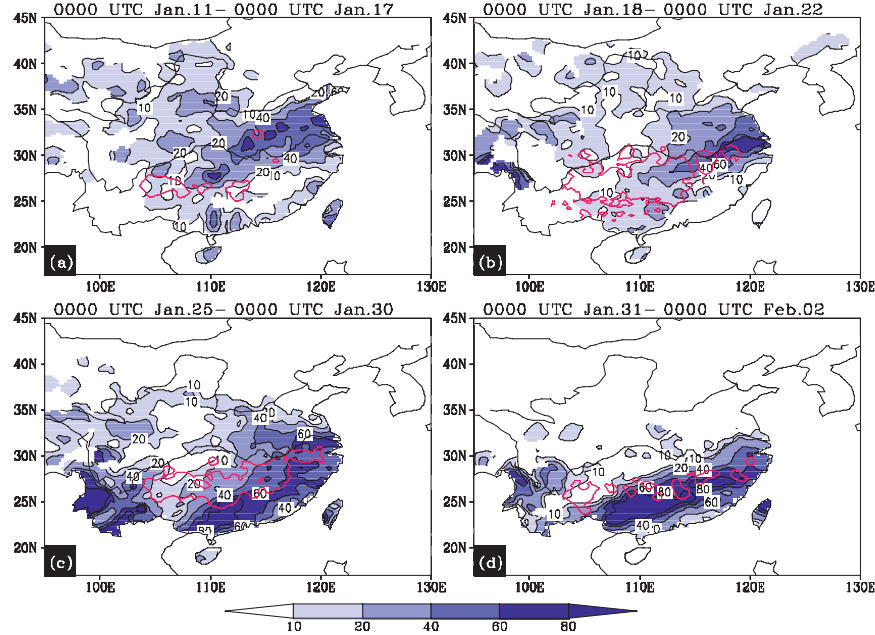


FIG. 3. The total precipitation amounts (shaded; mm) and freezing rain areas (enclosed by red line) during the four freezing precipitation stages from January to February 2008: (a) 0000 UTC 11 Jan–0000 UTC 17 Jan, (b) 0000 UTC 18 Jan–0000 UTC 22 Jan, (c) 0000 UTC 25 Jan–0000 UTC 30 Jan, and (d) 0000 UTC 31 Jan–0000 UTC 2 February.

The freezing precipitation and snowfalls from January to February 2008 present some significant and distinct synoptic characteristics, including a quasi-stationary front in south China that rarely occurs in wintertime. What has been understood is that the quasi-stationary front is typical during the Asian mei-yu season in summer from mid-June to mid-July over southern China and Japan (Tao and Chen 1987; Ding 1992), resulting in heavy rain and flash floods (Ding 1992; Zhao et al. 2004). In addition to the quasi-stationary front, the trough of the westerlies to the south of the Tibetan Plateau also played an important role in this pattern by transporting warm air and moisture to southern China. This paper studies the following three questions about the freezing precipitation during 2008 in China: 1) Is the 20-day-long persistence of the freezing precipitation event caused by the stable and anomalous atmospheric circulation? 2) What are the impacts of a quasi-stationary front on the formation of freezing precipitation and snowstorms? 3) Are surface properties and atmospheric stratification also important for the formation of freezing precipitation over southern China?

We address these three questions by analyzing relevant weather systems and mechanisms associated with this record-setting event, and present a conceptual model for improving our understanding of freezing precipitation events. Synoptic conditions of this long-duration event and the distribution of its freezing precipitation

are described in section 2. The quasi-stationary front, stratification, and surface conditions producing freezing precipitation and snowfall are diagnosed in section 3. The conceptual model for long-duration freezing precipitation is proposed in section 4. Finally, the conclusions and summary are presented in section 5.

2. The synoptic weather systems

Data from the $1^\circ \times 1^\circ$ National Centers for Environmental Prediction–National Center for Atmospheric Research (NCEP–NCAR) reanalysis were used to analyze the synoptic conditions during the course of this study. The 3-h surface observations are used to diagnose the geographic distribution of three types of freezing precipitation, including FZDZ, FZRA, and IPE. All of the observation data used in this study (e.g., 24-h precipitation amount, radiosonde data, and surface data in China) were provided by the China Meteorological Administration (CMA).

The disastrous weather, including heavy snowfall and freezing precipitation, began on 10 January and ended on 2 February 2008. This long duration can be divided into four stages. The main rainy area of the first stage (from 0000 UTC 11 January to 0000 UTC 17 January) was in the middle reaches of the Yangtze River, with freezing precipitation occurring over Guizhou and Hunan Provinces in southwestern China (Fig. 3a). Enclosed by the red line in

Fig. 3 are those areas in which all the weather stations reported freezing precipitation. The second stage was from 0000 UTC 18 January to 0000 UTC 22 January, when the heavy precipitation of more than 60 mm occurred in the middle and lower reaches of the Yangtze River. The areas of freezing precipitation were wider than that in the first stage and extended from southwestern China to the Yangtze River basin (Fig. 3b). The third stage was from 0000 UTC 25 January to 0000 UTC 30 January when the areas of freezing precipitation extended from southwestern China to the Yangtze River basin (Fig. 3c). In the fourth stage, from 0000 UTC 31 January to 0000 UTC 2 February, the center of the heavy precipitation zone was located to the south of the Yangtze River (Fig. 3d). Of the four stages, the second and the third had wider areas of the freezing precipitation, covering Guizhou, Hunan, Jiangsu, and Zhejiang Provinces (Fig. 3).

We discuss here the large-scale circulation, the characteristics of the surface conditions, and the stratification associated with each of these four stages. To better understand the maintenance and evolution of this long-duration freezing precipitation event, we also analyzed the geographic distribution, diurnal variations in freezing precipitation, and detailed information about the circulation during each stage.

a. The geographical distribution and diurnal variation of freezing precipitation

1) GEOGRAPHICAL DISTRIBUTION

Figure 4 shows the geographical distribution of FZDZ, FZRA, and IPE from 3-h surface observations from 10 January to 2 February. FZRA and IPE were observed from 22° to 28°N and from 104° to 123°E, covering an area from Guizhou Province in southwestern China to Zhejiang Province in eastern China (Fig. 4), but the FZDZ was found only in Guizhou Province. In contrast, FZRA occurred most frequently (more than 60 times in 23 days) in Guizhou and the Hunan Provinces, while IPE had a maximum occurrence of 20–40 times in the Hunan and Jiangxi Provinces. Of the three types of precipitation, FZRA was the most widespread and occurred most frequently in southern China.

A map of the daily number of stations reporting FZDZ, FZRA, and IPE (Fig. 5) shows that FZDZ occurred infrequently, and only two stations at most reported it at the same time. Hence, the following analysis concentrates on the study of the formation mechanisms of FZRA and IPE. FZRA occurred more frequently from 18 to 29 January than during the other stages in this study. The IPE falls into wider areas, and its occurrence was more frequent during 28–29 January and 1–2 February than during the other stages in this study.

2) DIURNAL VARIATION

A diurnal variation pattern was found in the surface observations for FZRA and IPE, but not for FZDZ (Fig. 6). The frequency of FZRA peaked at 2300–0800 Beijing standard time (BST = UTC + 8 h), then decreased sharply during the morning, and reached its minimum in the afternoon. In contrast, the diurnal variation of the frequency of IPE was not as strong and was in the opposite phase of that of FZRA; it peaked at 1400 BST, decreased during the afternoon, and reached a minimum at 2000 BST. There was no apparent diurnal change for FZDZ, perhaps due to its infrequent occurrence.

Cortinas et al. (2004) studied the climatology of the diurnal distribution of freezing precipitation from 1976 to 1990. They found that FZRA and FZDZ occurred most often just before sunrise and had their lowest frequencies near sunset, whereas the frequency of IPE was nearly constant throughout the day. Cortinas et al. (2004) also indicated that the rapid decrease in frequency of FZRA near sunrise was a result of precipitation cessation and conversion to rain. The diurnal variation of FZRA in southern China is similar to that in North America. But, the diurnal variation of IPE is stronger in southern China when compared to the nearly constant results found for North America. Since the results of Cortinas et al. (2004) are a climatologic diurnal distribution, while this study only used data from 20 days during 2008, in future studies we plan to conduct climatologic analyses of IPE in China to further compare with the results of Cortinas et al. (2004).

b. The synoptic patterns in the four stages

Figures 7 and 8 show the average geopotential height and anomalies at 500 hPa, the average wind, and the temperature fields at 850 hPa for the four freezing precipitation stages, respectively. Figure 7a indicates that the westerlies in the first stage could be seen forming two branches: one to the north of 40°N (north branch) and the other to the south of 40°N (south branch). A blocking high existed in the north branch of the westerlies, and the high pressure system was located from near Lake Baikal to western Siberia. On the east and west sides of this blocking high were both low pressure systems. The significant positive and negative anomalies of the geopotential height at 500 hPa appeared at the locations of the blocking high and the low pressure system to its east, respectively. The low pressure system in eastern Mongolia and northeastern China was favorable for the cold air to move into southern China. The large-scale troughs stagnated over Yunnan Province and the northern Indochina peninsula. However, the small-amplitude troughs, which split from the large-scale trough

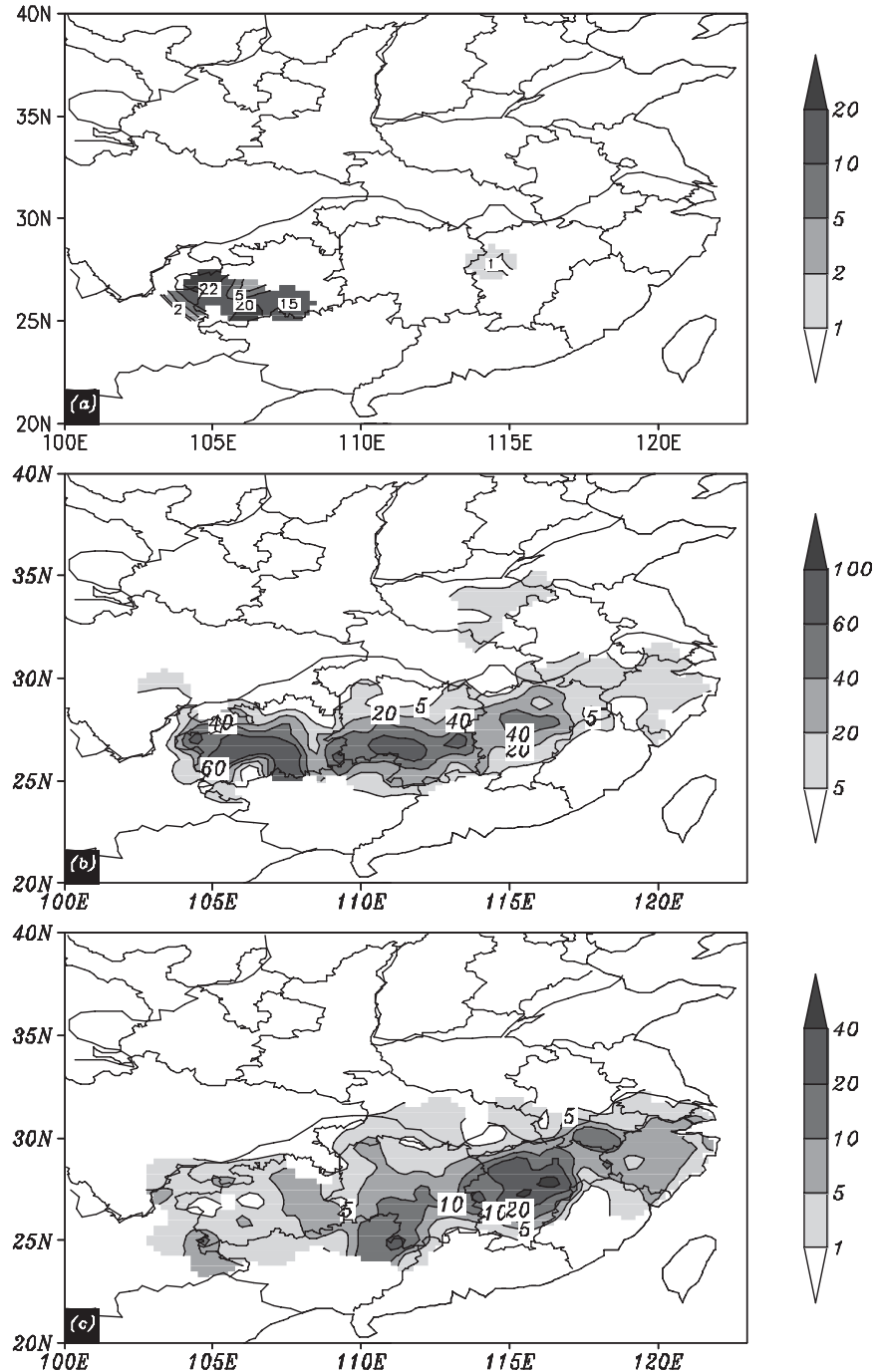


FIG. 4. Total number of reports from 3-hourly surface observations (number) for (a) freezing drizzle, (b) freezing rain, and (c) ice pellets from 10 Jan to 2 Feb 2008. Each panel uses a different scale, with intervals of 1, 2, 5, 10, and 20 in (a); intervals of 5, 20, 40, 60, and 100 in (b); and intervals of 1, 5, 10, 20, and 40 in (c).

at 500 hPa, continually moved eastward along the south branch of the westerlies and transported abundant moisture toward southern China. The most distinct characteristic in the wind field at 850 hPa (Fig. 8a) was the

maintenance of a shear line related to a quasi-stationary front along the Yangtze River basin (the temperature and pseudo-equivalent potential temperature fields will be analyzed in section 3); such a significant shear line in

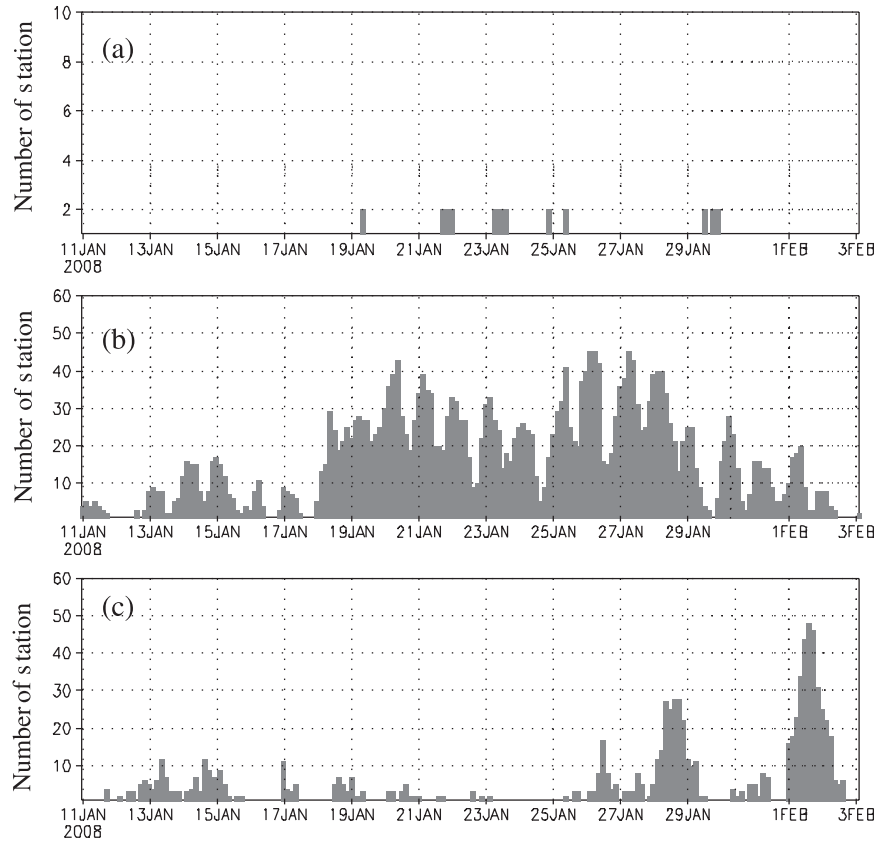


FIG. 5. The time series of the reported numbers of stations at 3-h observations for (a) freezing drizzle, (b) freezing rain, and (c) ice pellets from 10 Jan to 2 Feb 2008.

a wind field is rare during winter in China. Hence, the maintenance of the quasi-stationary front along the Yangtze River basin was instrumental to the formation and long duration of the rain-snow band in southern China, although the FZRA occurred only in Guizhou and Hunan Provinces during this stage (Fig. 3a).

The precipitation during the second stage, from 0000 UTC 18 January to 0000 UTC 22 January, was also mainly in the Yangtze River basin, and the occurrence of the freezing precipitation greatly aggravated disaster recovery efforts (Fig. 3b). The average circulation at 500 hPa shows a blocking high pressure developing near the Ural Mountains (Fig. 7b). To the south of it, an east-northeast-west-southwest-extending trough was maintained from Lake Baikal to the Caspian Sea and then the Aral Sea. A cutoff low appeared on the east side of the Caspian Sea and the Aral Sea, which favored the maintenance of the trough in the southern branch of the westerlies. When compared with the climatology, the areas of the blocking high pressure and the cutoff low in this period showed the positive and negative pressure anomalies, respectively.

The wind field at 850 hPa (Fig. 8b) showed that the cold air moved southward from the Yangtze River basin

toward South China during this stage (the track of cold air marked in Fig. 8). At the same time, the transport of moisture from the western Pacific Ocean, the South China Sea, and the Bay of Bengal was also enhanced.

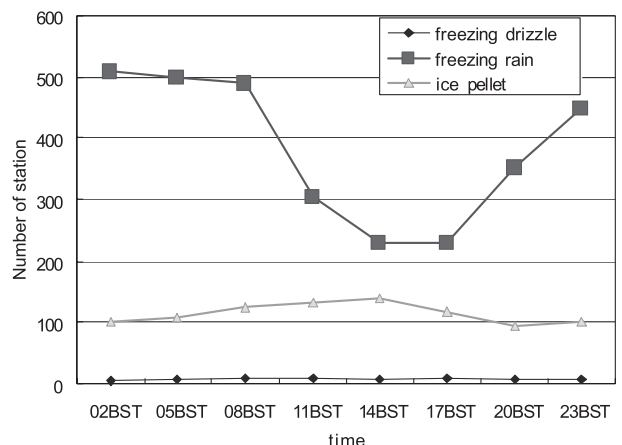


FIG. 6. The diurnal variation of freezing drizzle, freezing rain, and ice pellets in 3-h surface observations from 10 Jan to 2 Feb 2008.

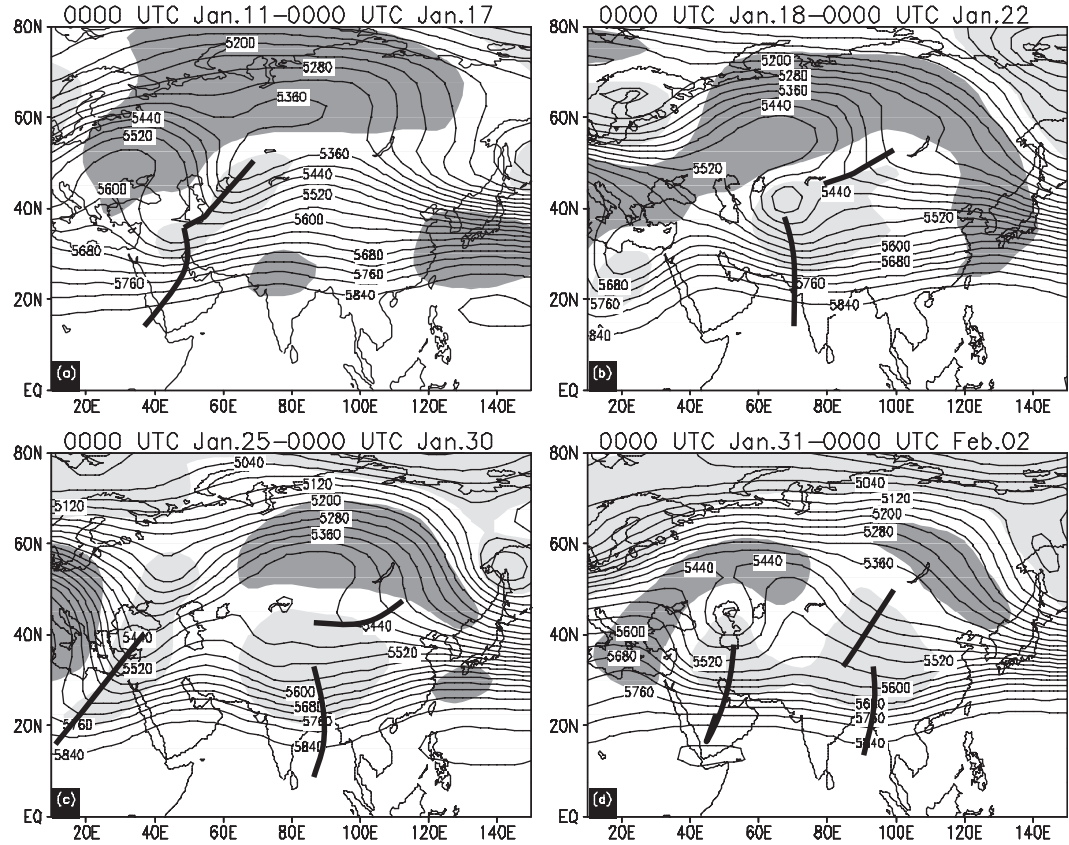


FIG. 7. The average geopotential height and anomalies (gpm; dark shading is for positive anomalies >50 gpm, and light shading is for negative anomalies ≤ 50 gpm) at 500 hPa of the following four freezing precipitation stages from January to February 2008, with a black boldface line for the trough axis: (a) 0000 UTC 11 Jan–0000 UTC 17 Jan, (b) 0000 UTC 18 Jan–0000 UTC 22 Jan, (c) 0000 UTC 25 Jan–0000 UTC 30 Jan, and (d) 0000 UTC 31 Jan–0000 UTC 2 Feb.

Consequently, a shear line in the wind field and a quasi-stationary front in the temperature field were formed and maintained over southern China.

The third stage showed quite different features from the second. A rainband first appeared in southern China and then moved northward to the Yangtze River basin, but the area of freezing precipitation still remained mainly over Hunan and Guizhou Provinces and only extended toward eastern China in the later stages. A blocking high was still maintained near western Siberia, ahead of an east–west-directed trough over northern China. In the southern branch of the westerlies, southern China was to the east of the India–Burma trough, where a convergence zone of moisture was transported by the trough (Fig. 7c). At 850 hPa (Fig. 8c), the shear line and a quasi-stationary front were located to the south of the Yangtze River. Although the quasi-stationary front shifted between the Yangtze River basin and southern China during this stage, the area of freezing precipitation was mainly over Guizhou and Hunan Provinces

and only expanded toward Jiangxi and Jiangsu Provinces in the later stages.

During the fourth stage, the precipitation between 31 January and 2 February mainly occurred over southern China and to the south of the Yangtze River (Fig. 3d). The main circulation pattern during this stage was similar to that during the third stage, except that the blocking high near western Siberia was weakened and the shear line moved toward southern China (Figs. 7d and 8d). As a result of the circulation adjustment, especially the eastward movement and the decay of the blocking high, the whole precipitation process was finished (not shown).

In summary, the general circulation between 10 January and 2 February 2008 showed unique synoptic characteristics during boreal winter with the persistence of the blocking high pressure in the north branch of the westerlies, the shear line, and a quasi-stationary front between the Yangtze River basin and southern China, which resulted in a very favorable environment for the formation and development of the severe rain–snow event.

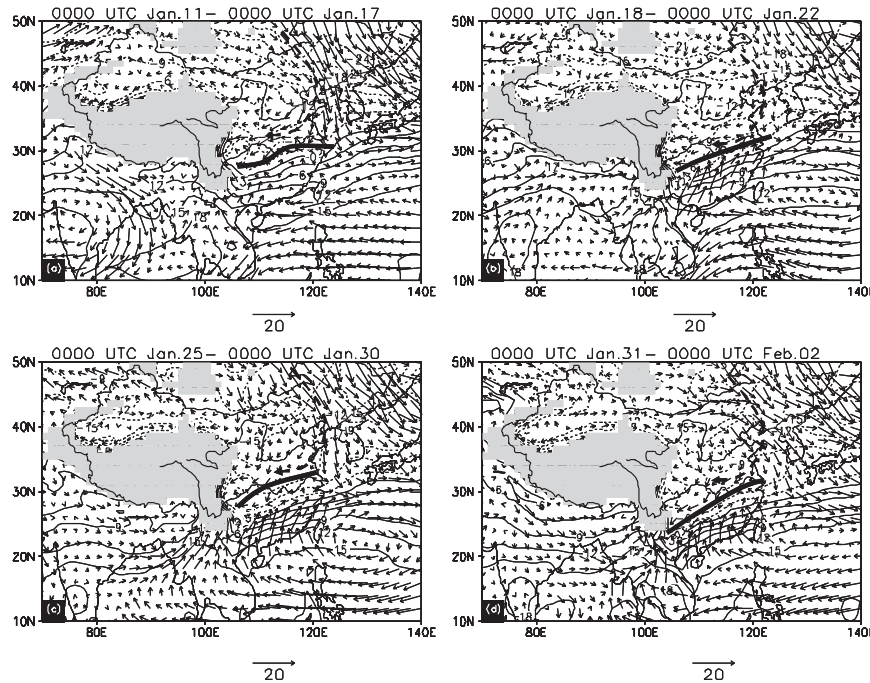


FIG. 8. The average wind at 850 hPa (m s^{-1}) and temperature ($^{\circ}\text{C}$; thin solid line $>0^{\circ}\text{C}$ and thin dashed line $\leq 0^{\circ}\text{C}$) of the following four freezing precipitation stages from January to February 2008, with a black boldface line for the shear line, a boldface dashed line for the track of the cold air, and with shading representing terrain >1500 m: (a) 0000 UTC 11–0000 UTC 17 Jan, (b) 0000 UTC 18 Jan–0000 UTC 22 Jan, (c) 0000 UTC 25 Jan–0000 UTC 30 Jan, and (d) 0000 UTC 31 Jan–0000 UTC 2 Feb.

c. The eastward propagation of cloud systems from the Tibetan Plateau

Tao and Ding (1981) indicated that the Tibetan Plateau can exert very important effects on the initiation and development of heavy rainfall and severe storms in China. Many rain-bearing synoptic systems have their origins over the plateau and then move eastward or northeastward to cause excessively heavy rains in eastern and northern China. Further, Jiang and Fan (2002) pointed out that the activities of mesoscale convective systems (MCSs) over the plateau during the summer of 1998 were mainly to the southeast and southwest of the Tibetan Plateau, but only a few of these systems can move eastward and influence the middle and lower reaches of the Yangtze River basin. Zhang et al. (2002) proposed a multiscale model of the rainstorms causing flash flooding in the Yangtze–Huaihe basin. They suggested that the eastward movement of meso- α -scale systems over the Tibetan Plateau to the Yangtze–Huaihe basin could be a trigger for the formation and development of meso- α -scale convective systems along the mei-yu front. Yasunari and Miwa (2006) presented detailed analysis of the convective system activities over the Tibetan Plateau and found that those systems moving eastward from the plateau may

have caused the development of mesoscale convective cloud clusters along the mei-yu front region in 1998.

During the long-duration rain and snow event in early 2008, the synoptic layout of a shear line and a quasi-stationary front, to some extent, was very similar to that of the summer mei-yu front. Now the question is, Did the mesoscale systems over the plateau also show persistent impacts in the continuous rain–snow process? To answer this question, infrared data for cloud-top temperatures from the Chinese Fēngyún (FY-2C) satellite have been used to analyze the activities of mesoscale systems propagating eastward from the Tibetan Plateau toward eastern China. Data with a horizontal resolution of 0.05° were available every hour and covered the whole of East Asia (20° – 70° N, 70° – 160° E). The temporal evolution of the hourly average cloud-top temperature and 6-h precipitation amounts between 22° and 35° N from 10 January to 3 February were shown in Fig. 9. When compared with the cloud activity patterns after 18 January, the cloud clusters were not very active over the plateau before 17 January. A weak convective system propagating eastward from the plateau influenced the region to the east of 110° E (Fig. 9a), which corresponded to the relatively strong precipitation on 18 January (Fig. 9b). After 21 January, the cloud clusters over the Tibetan Plateau were

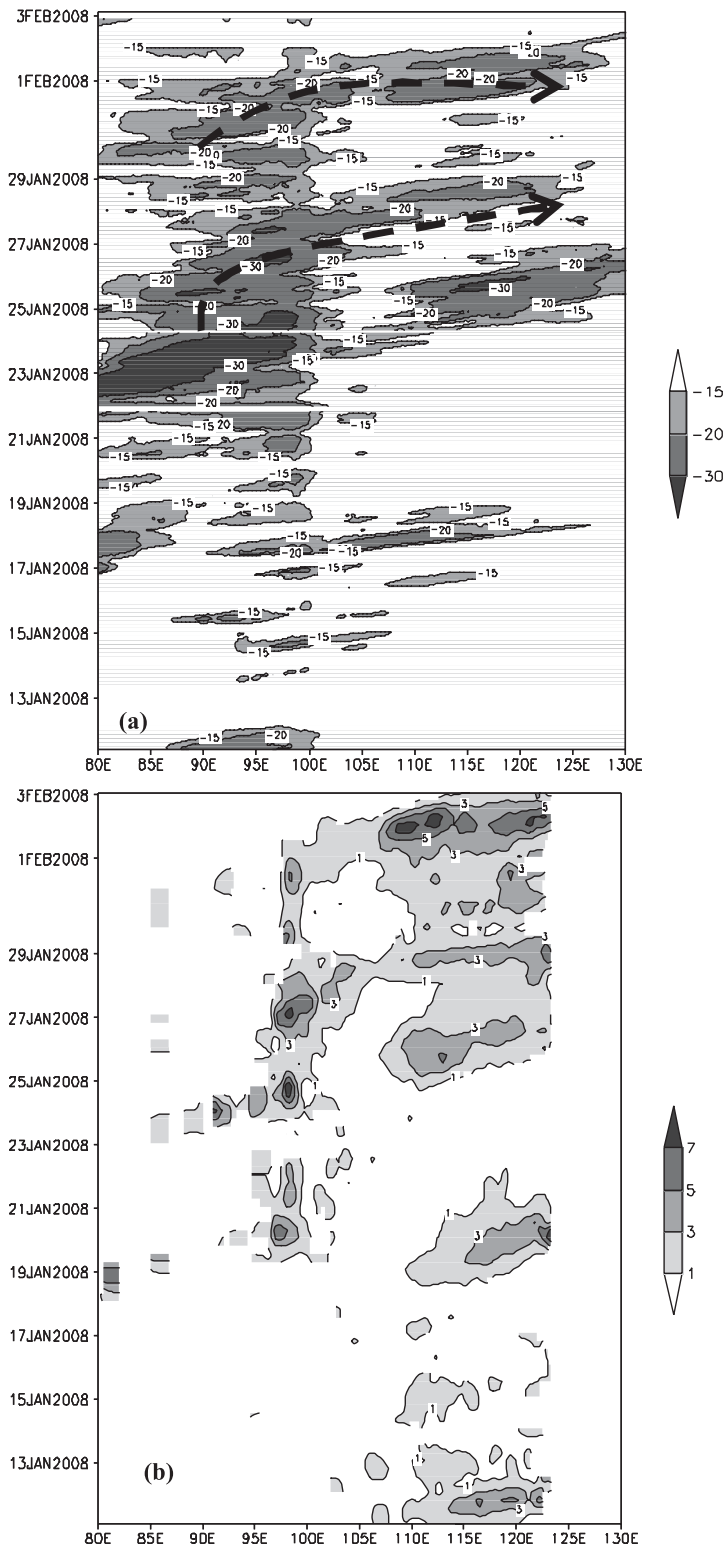


FIG. 9. Time-lon cross sections of (a) satellite-derived average cloud-top temperature ($^{\circ}\text{C}$, shading begins at -15°C , with intervals of 5°C) over 80° – 130°E from 11 Jan to 3 Feb 2008 and (b) average precipitation amount (mm, shading begins at 1 mm) over 80° – 130°E from 11 Jan to 3 Feb 2008. The boldface dashed line shows the eastward propagation of systems from the Tibetan Plateau.

very active, but did not move eastward until 26 January. These systems affected the middle and lower reaches of the Yangtze River from 27 to 29 January (Fig. 9a), leading to the heavy precipitation from 27 to 28 January (Fig. 9b). The systems over the plateau became weaker after 29 January, but were still relatively active, then moved eastward from 31 January to 1 February (Fig. 9a) and induced the strong precipitation on 1–2 February (Fig. 9b).

The eastward propagations of these cloud clusters from 26 to 28 January were selected for further detailed analysis here (Fig. 10). These propagations occurred at three different periods. The first propagation occurred several hours after 0000 UTC 26 January when a cloud cluster over the southeastern Tibetan Plateau (30°N , 95°E) developed, and this cloud cluster propagated northeastward without affecting southern China. However, the second propagation event happened on 25 January, when the cloud cluster north of 30°N over the plateau moved out across the plateau; it started influencing the Yangtze River basin and reinforced the rainfall at 2100 UTC on 26 January. The third propagation event took place at 0000 UTC 27 January, and the movement of the cloud clusters was similar to that in the first propagation event, except that the track was located more southward, and thereby influenced the Yangtze River basin.

As discussed in section 2, the persistent rain–snow weather pattern in early 2008 had four phases: 11–17 January, 18–22 January, 25–30 January, and 31 January–2 February. With the exception of the first phase, the remaining three phases were accompanied by the eastward movement of cloud clusters from the plateau. This might explain why the precipitation was the weakest during the first stage (Fig. 9b).

3. The characteristics of the atmospheric conditions associated with freezing precipitation

Freezing precipitation forms through two microphysical paths: melting processes and supercooled warm rain processes (Rauber et al. 2000). The melting occurs when ice particles fall from the middle level into a lower-tropospheric level, where the air temperature exceeds 0°C . The ice particles melt into raindrops within the layer, then fall into a subfreezing surface layer, supercool, and freeze on contact with surface objects. The supercooled warm rain process acts via the collision and coalescence of droplets. Although the formation of freezing precipitation normally exists in microphysical paths regardless of the occurrence of a warm layer aloft, FZRA and IPE usually require an elevated warm layer and a subfreezing surface layer below.

Numerous investigators have shown that this thermal stratification in North America can occur primarily as

a result of airflow associated with extratropical cyclones and topographical effects (Bernstein 2000; Rauber et al. 2000; Stewart and King 1987; Stewart 1992). Now the question is, Which system led to the formation of the observed thermal stratification over southern China from 11 January to 2 February 2008? The third stage (25–30 January) was selected here as an example to analyze the characteristics of the quasi-stationary front. The surface and radiosonde records of the whole period were used to document the surface conditions and stratification associated with the freezing precipitation process.

a. The quasi-stationary front

A quasi-stationary front in either the east–west or northeast–southwest directions was formed during this freezing precipitation stage, over southern China and sometimes along the Yangtze River basin. This was an important feature for producing freezing precipitation. Generally, an east–west front in southern China formed between the cold air from the north and warm air from the south, so sometimes, a shear line between the northerly and southerly winds could be found in the wind field of the lower troposphere. During this freezing precipitation, a shear line in the wind field at 850 hPa, related to the frontal zone (strong gradient of temperature), can also be clearly found (Fig. 8), but such quasi-stationary fronts seldom appeared during the winter in southern China.

IPE, FZRA, and rain during this stage mainly occurred in the western part of the quasi-stationary front (west of 116°E), while snow, IPE, and rain mainly appeared in the eastern part (east of 116°E). Here, the differences between the frontal surface's eastern and western parts were studied through vertical cross-sectional analysis. In the transition region bounded by snow on one side and rain on the other, Stewart (1992) found that the precipitation can be in the form of snow mixed with rain, or that it can contain FZRA and IPE. Therefore, a better understanding of the precipitation type in the transition region is important for improving predictions of winter precipitation.

Figure 11 depicts the vertical cross section of the pseudo-equivalent potential temperature (θ_{se}) at 0000 UTC from 26 to 28 January along 113°E , representing the western part of front, and along 119°E , representing the eastern part of front. The θ_{se} and moisture flux were calculated by using NCEP–NCAR reanalysis data. Here, θ_{se} is defined by lifting an air parcel upward along a moist pseudo-adiabatic trajectory, extracting all water vapor, and returning adiabatically to the surface (Tao 1980), which can be calculated as $\theta_{\text{se}} = T(1000/P)^{R_d/c_p} \exp(Lq/c_p T)$, where T , q , and L are the temperature, specific humidity, and latent heat, respectively; and R_d

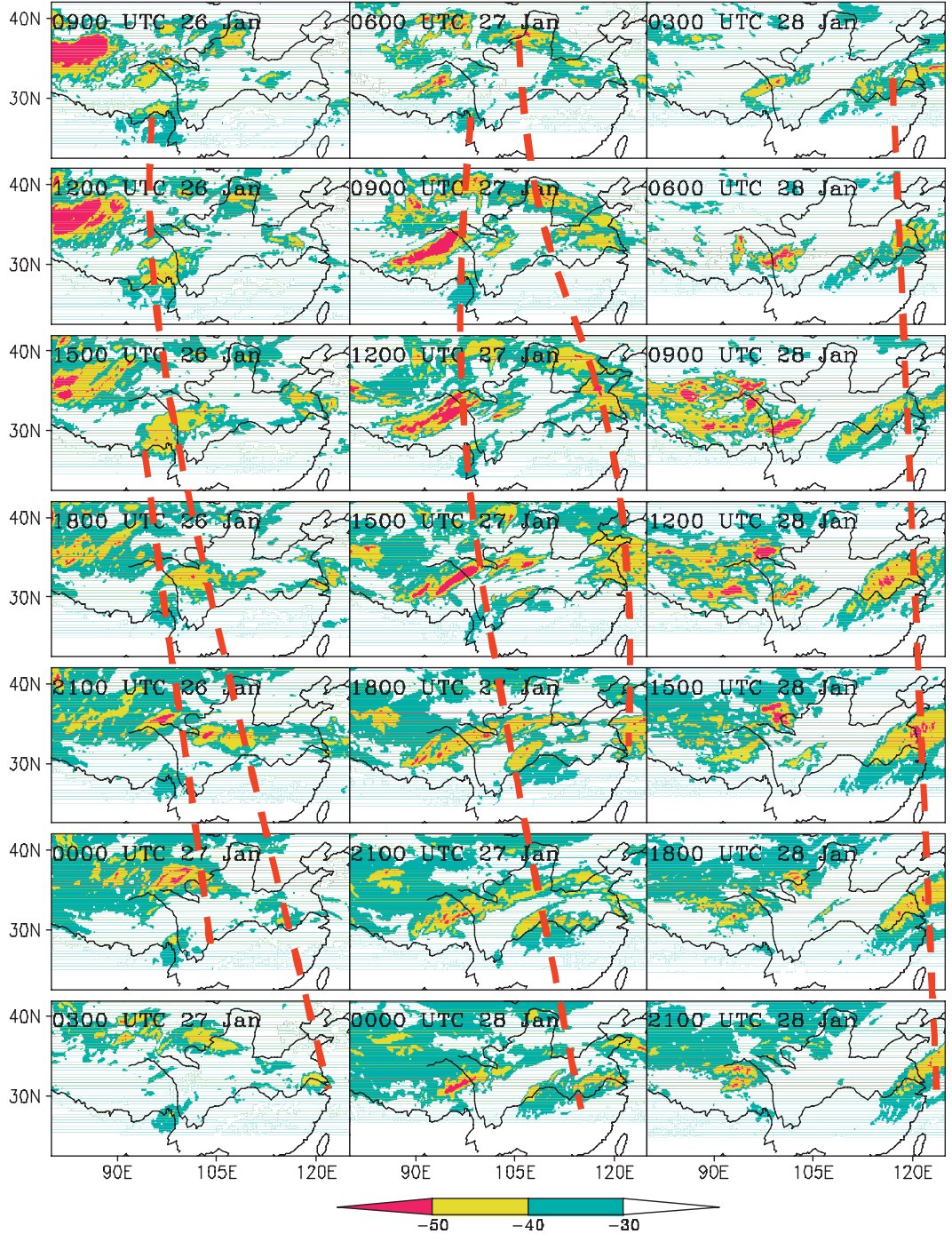


FIG. 10. Time series of satellite-derived cloud-top temperature ($^{\circ}$ C) images at 3-h intervals from (top left) 0900 UTC 26 Jan to (bottom right) 2100 UTC 28 Jan 2008. The boldface red dashed lines show the eastward propagation of the convective cloud areas originating over the Tibetan Plateau.

and c_p are the specific gas constant of dry air and the specific heat at constant pressure of dry air, respectively.

The frontal zone was characterized by a larger horizontal gradient between the two isolines (280–320 K) of θ_{se} . The western part of the front was about 500 km in

width on the ground (Figs. 11a–c), while the eastern part of the front was about 700 km (Figs. 11d–f). The isolines of θ_{se} were denser in the western part of the front than that in the eastern part, which means that the temperature gradient of the western front in the middle–lower

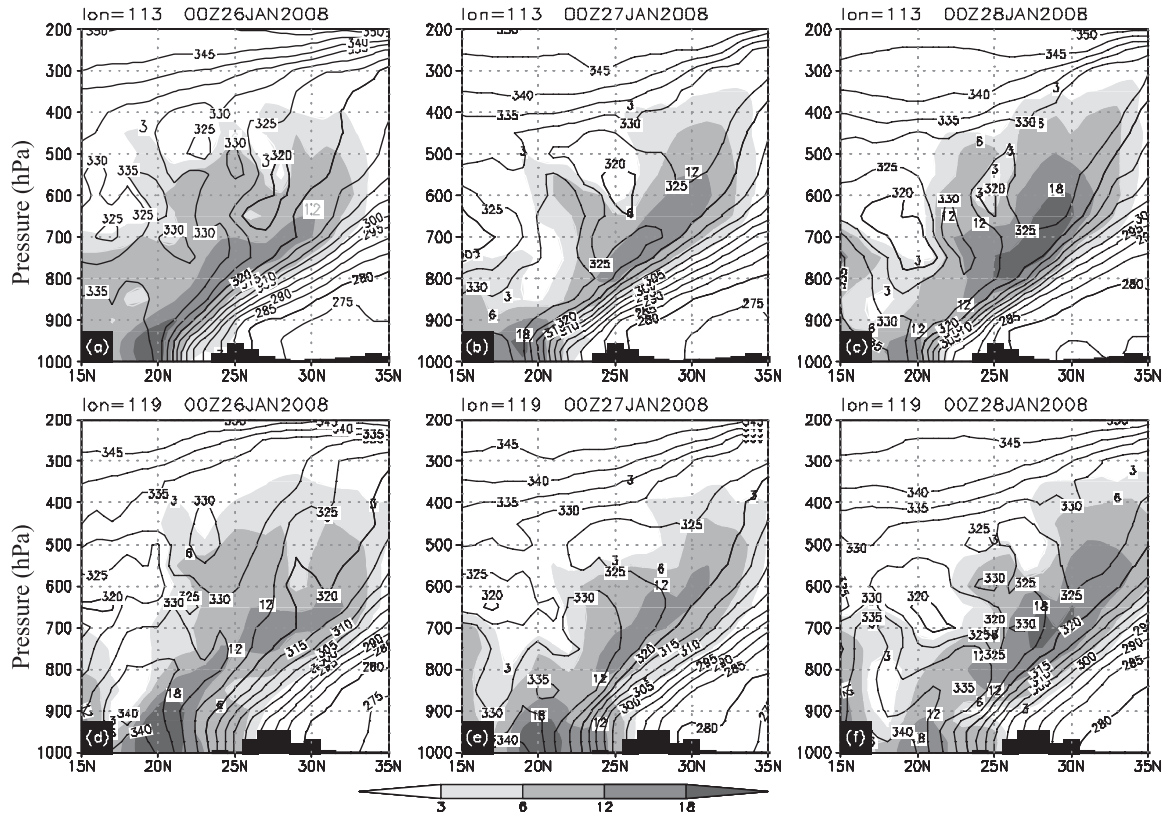


FIG. 11. Vertical cross section of the pseudo-equivalent potential temperature (solid, K) and moisture flux (shading; $\text{g s}^{-1} \text{cm}^{-1} \text{hPa}^{-1}$) along (top) 113° and (bottom) 119°E from 0000 UTC 26 Jan to 0000 UTC 28 Jan 2008, with dark shading representing the terrain: (a),(d) 0000 UTC 26 Jan, (b),(e) 0000 UTC 27 Jan, and (c),(f) 0000 UTC 28 Jan 2008.

troposphere was stronger. The warm moisture air converged along the front zone. The convergence also was stronger in the western part of the front than that in the eastern part (Figs. 11 and 12). The FZRA in the western part of the front occurred over Guizhou and Hunan Provinces and ranged from 25° to 28°N (Figs. 11a–c); primarily, the FZRA area was to the north of the surface front zone. However, in the eastern front, snow occurred to the north of the surface front and rain appeared near the front zone and to the south of it (Figs. 11d–f). FZRA forms generally at surface temperatures of 0°C or below. The vertical distribution of the temperature (Fig. 12) shows that the 0°C isotherm of the surface temperature was around 25°N in the western part of front (Figs. 12a–c), and ranged from 28° to 30°N in the eastern part of front (Figs. 12d–f). The main reason for the differences in precipitation type between the western and eastern parts of the front was the different atmospheric stratification conditions in the middle–lower troposphere. In the western part of the front, from 25° to 28°N , there was a deep inversion with a 5° – 8°C increase from 950 to 700 hPa, and a warmer layer ($>0^\circ\text{C}$) between 900 and 600 hPa (Figs. 12a–c). Such a distribution of the lapse

rate, as discussed in Rauber et al. (2000), was favorable for the formation of FZRA because 1) in the middle troposphere there is a freezing layer, 2) below the freezing layer there is a warm layer (melting layer) and an inversion, and 3) close to surface there is a thin layer with temperatures less than 0°C . However, similar vertical structures in temperature were not found in the eastern part of the front (Figs. 12d–f). Therefore, freezing rain did not appear in the eastern part of the front, and its 0°C isotherm at the surface was indeed the boundary between the rain and the snow areas.

To discuss the influences of frontogenesis on the quasi-stationary front, the frontogenetical function was calculated by using following equations:

$$\begin{aligned}
 F = \frac{d}{dt} |\nabla \theta| &= \frac{1}{|\nabla \theta|} \left[(\nabla \theta) \cdot \nabla \left(\frac{d\theta}{dt} \right) \right] - \frac{1}{2} \frac{1}{|\nabla \theta|} (\nabla \theta)^2 D_h \\
 &\quad - \frac{1}{2} \frac{1}{|\nabla \theta|} \left\{ \left[\left(\frac{\partial \theta}{\partial x} \right)^2 - \left(\frac{\partial \theta}{\partial y} \right)^2 \right] A_f \right. \\
 &\quad \left. + 2 \frac{\partial \theta}{\partial x} \frac{\partial \theta}{\partial y} B_f \right\} - \frac{1}{|\nabla \theta|} \frac{\partial \theta}{\partial p} \left(\frac{\partial \theta}{\partial x} \frac{\partial \omega}{\partial x} + \frac{\partial \theta}{\partial y} \frac{\partial \omega}{\partial y} \right),
 \end{aligned}$$

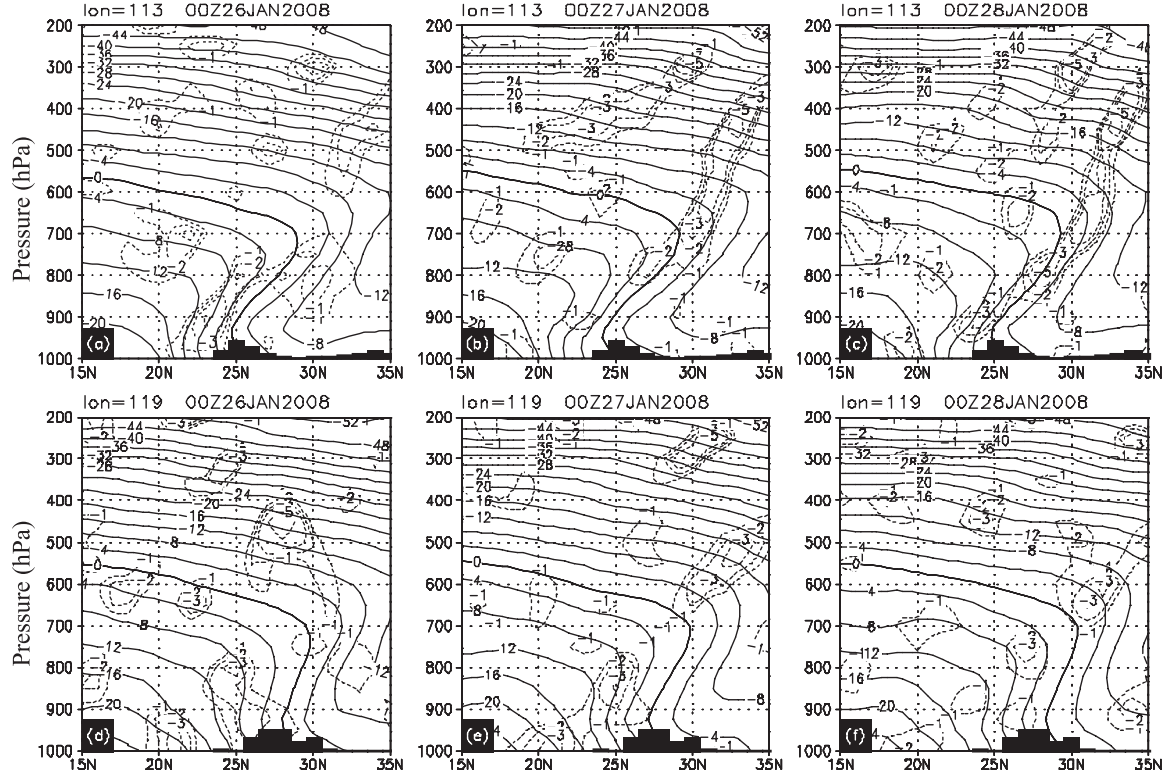


FIG. 12. Vertical cross sections of temperature (solid; $^{\circ}\text{C}$) and divergence (dashed line; 10^{-5} s^{-1}) along (top) 113° and (bottom) 119°E from 0000 UTC 26 Jan to 0000 UTC 28 Jan 2008, with dark shading representing the terrain: (a),(d) 0000 UTC 26 Jan, (b),(e) 0000 UTC 27 Jan, and (c),(f) 0000 UTC 28 Jan 2008.

where

$$A_f = \frac{\partial u}{\partial x} - \frac{\partial v}{\partial y}, \quad B_f = \frac{\partial v}{\partial x} + \frac{\partial u}{\partial y}, \quad \text{and} \quad D_h = \frac{\partial u}{\partial x} + \frac{\partial v}{\partial y}.$$

Here, F is the frontogenetical function, which is defined as the variation ratio with time of the horizontal gradient of a specific meteorological parameter, for example, potential temperature (Keyser and Shapiro 1986). In addition, u and v are the horizontal wind velocity components, and θ is the potential temperature.

Figure 13 shows the vertical cross section of the frontogenetical function along 113° and 119°E , respectively. The frontogenetical area was vertically deeper in the alongfront zone and its maxima appeared below 700 hPa (Fig. 13). The frontogenesis was stronger in the western part of the front than that in the eastern part, which could explain the fact that the horizontal gradient of θ_{se} in the western part of the front was stronger than that in the eastern part. It indicated that the baroclinity associated with the frontal zone played an important role during the freezing rain. The convergence along the front (Fig. 12) indicated that the warm air from the south was transported to where the front was located, which intensified the frontogenesis.

The analysis above indicates that the strong frontal zone in the western part of the front strengthened the inversion layer and the warm layer, which was favorable for the formation of FZRA. But the inversion in the eastern part of the front was weaker or absent a warm layer ($>0^{\circ}\text{C}$), which was unfavorable to the formation of FZRA.

b. The surface conditions

The 3-h surface temperature, dewpoint temperature, and wind field from 17 to 30 January were analyzed to help us better understand the impacts of the surface conditions on the FZRA and IPE. The horizontal distribution of the precipitation type and surface temperature reveals that freezing precipitation appeared in the region where the surface temperature was between 0° and -3°C . The freezing precipitation area is about 200–300 km in width, to the north of 0°C isotherm at surface.

A statistical study of freezing precipitation data from 1928 to 2001 in the United States found that most FZRA occurred at dry-bulb temperatures of -2.2° to 0°C and dewpoint temperatures of -2.8° to -0.6°C (Houston and Changnon 2007). Figure 2 shows the distributions of the following eight sounding stations over the freezing

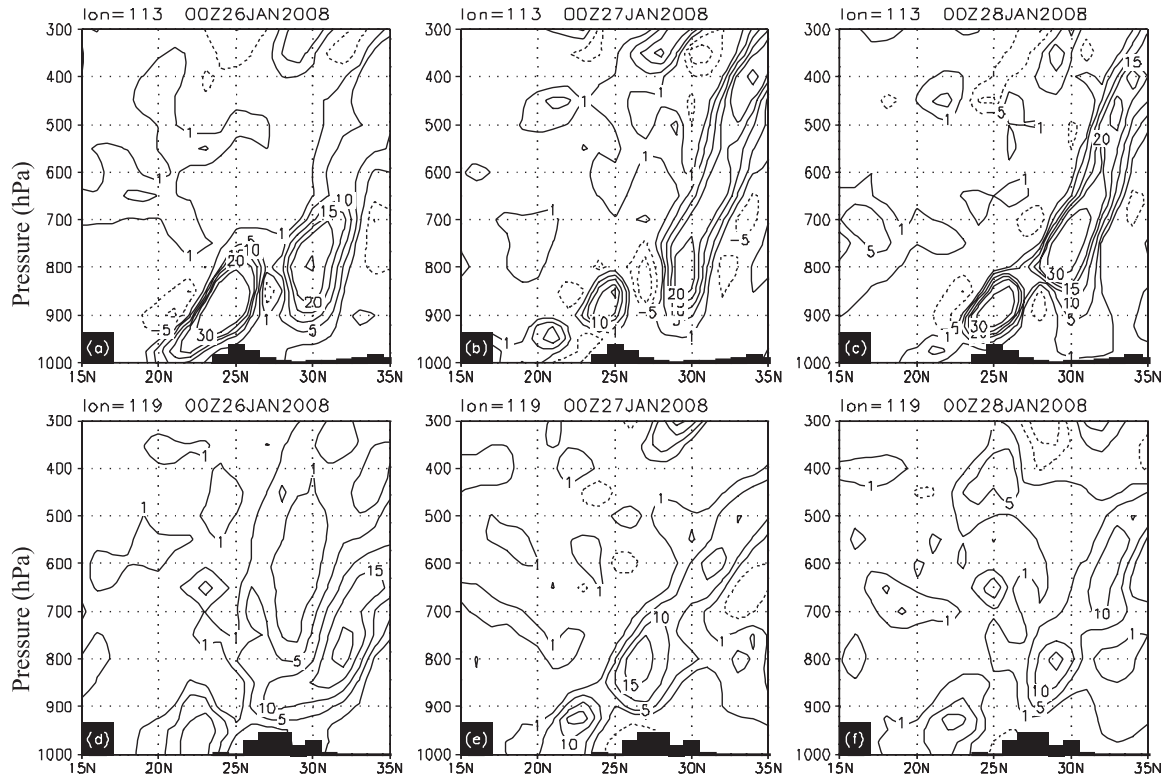


FIG. 13. Vertical cross sections of frontogenetical function (solid; $10^{-10} \text{ K s}^{-1} \text{ m}^{-1}$) along (top) 113° and (bottom) 119°E from 0000 UTC 26 Jan to 0000 UTC 28 Jan 2008, with dark shading representing the terrain: (a),(d) 0000 UTC 26 Jan, (b),(e) 0000 UTC 27 Jan, and (c),(f) 0000 UTC 28 Jan 2008.

precipitation area: Weining, Guiyang, Huaihua, Changsha, Chenzhou, Ganzhou, Nanchang, and Nanjing. In Chenzhou, Ganzhou, and Nanjing, freezing precipitation occurred infrequently and the elevation of 2236 m at Weining is too high to composite with the other stations. Thus, only Guiyang, Huaihua, Changsha, and Nanchang were selected to diagnose surface and sounding features.

Figure 14 shows the surface temperatures, dewpoint temperatures, wind fields, and weather phenomena at Huaihua, Changsha, Guiyang, and Nanchang from 17 to 30 January. The times of occurrence for freezing precipitation at these stations are listed in Table 1. The surface temperature during the freezing precipitation was -2° to -6°C at Guiyang, and -1° to -3°C at the other stations. The dewpoint depression ranged from 1° to 3°C for all stations, and was lower than 2°C at most stations. This indicates that the air near the surface was very moist with temperatures below 0°C , which was favorable to the formation of freezing precipitation. Generally, the surface wind direction was to the north or northeast and the wind speed was $0\text{--}4 \text{ m s}^{-1}$. In addition, the analysis of the relation between precipitation amount and precipitation type found that precipitation amounts during freezing precipitation were small. This

finding is consisted with the results of Houston and Changnon (2007).

In general, the surface temperature was favorable for the occurrence of freezing precipitation between -1° and -3°C and for the dewpoint depression the range was 1° to 3°C . However, the surface temperature during the freezing precipitation over the plateau is slightly lower than -3°C . At the same time, low wind speeds with relatively light precipitation amounts were common conditions during freezing precipitation events over southern China in January 2008. However, we also found that the surface conditions during the snowfall were quite similar to those during freezing precipitation. Therefore, surface conditions alone are not sufficient to determine the precipitation type, and other factors such as the stratification can also affect the precipitation type (Zerr 1997; Cortinas et al. 2004), which will be discussed in the next subsection.

c. The stratification associated with freezing precipitation

Table 2 lists the locations of the radiosondes where freezing precipitation was reported. Since the elevation of Guiyang is much higher than those of the other three stations, Guiyang and the other stations' soundings were

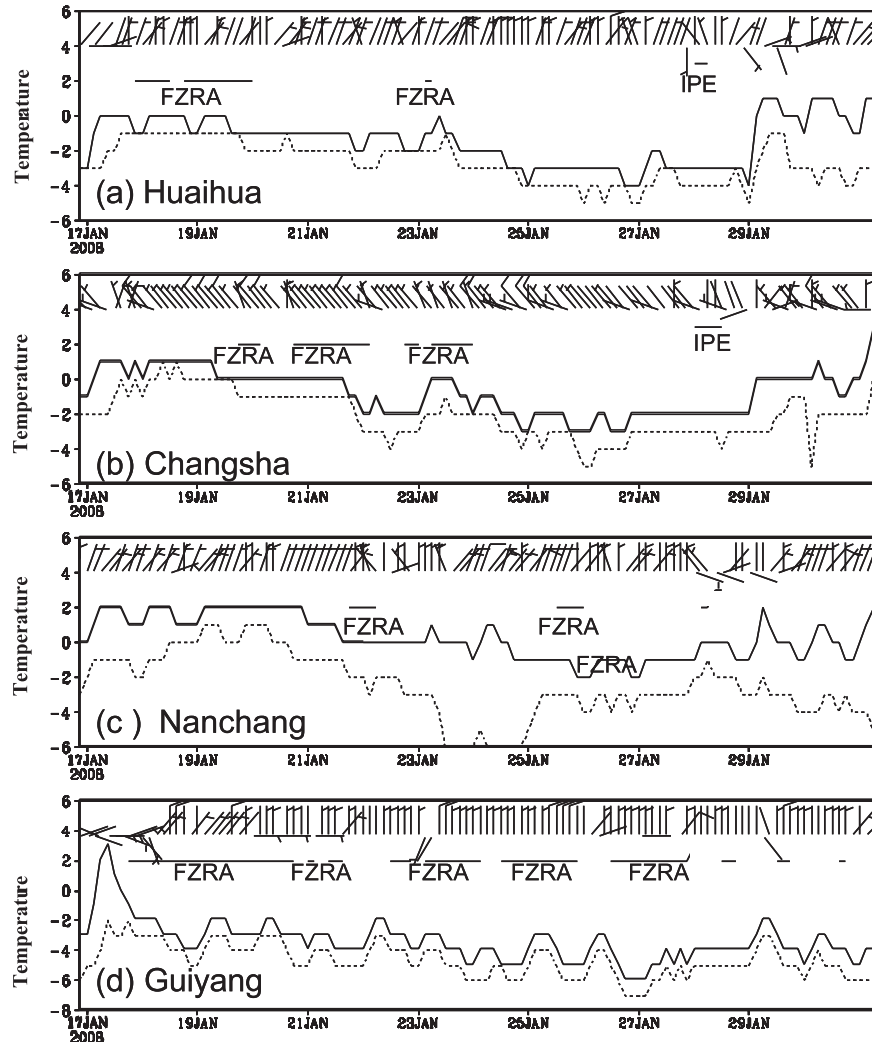


FIG. 14. Time series of 3-h surface observations from 17 to 30 Jan 2008 for (a) Huaihua; (b) Changsha, (c) Nanchang, and (d) Guiyang Provinces. Temperature (solid line; $^{\circ}\text{C}$), dew-point temperature (dashed line; $^{\circ}\text{C}$), and winds (half barb, 2.5 m s^{-1} ; full barb, 5.0 m s^{-1}). Periods of FZRA and IPE are marked with horizontal lines.

composite separately. As has been noted, FZRA was typically characterized by an above-freezing layer, an upper-level inversion, and a lower-level subfreezing layer (Stewart and King 1987).

Figure 15 shows composite soundings for IPE and FZRA. Here, the “cloud top” was defined as the first level above the low-level cloud layer where the dewpoint depression exceeded 3°C , provided that the dewpoint depression remained through a layer of at least 1-km depth (Rauber et al. 2000). The composite soundings for

IPE (Fig. 15a) were made from four radiosonde observations with mandatory and significant levels (Table 2) including one from Huaihua, two from Changsha, and one from Nanchang. These soundings showed that the cloud top was much higher than the warm layer ($>0^{\circ}\text{C}$) at about 500 hPa, with cloud-top temperatures of -20° to -10°C and a warm layer located at 700–800 hPa. The composite hodograph suggests a synoptic pattern with low-level northeasterly or easterly winds, and southwesterly winds aloft, indicating warm advection and

TABLE 1. Dates of freezing precipitation at specific radiosonde sites.

Name of radiosonde site	Guangzhou	Huaihua	Changsha	Nanchang
Dates of freezing precipitation (January)	18–20, 22–23, 25–29	18–20, 23, 28	20, 21–22, 23, 28	22, 26, 28

TABLE 2. Locations of radiosonde sites associated with observations of surface freezing precipitation.

Radiosonde site	Location	Altitude (m)	No. of cases	
			FZRA	IPE
Guiyang	26°35'N, 106 °43'E	1074	17	
Huaihua	27°34'N, 110 °00'E	261	6	1
Changsha	28°12'N, 113 °05'E	45.7	8	2
Nanchang	28°36'N, 115 °55'E	45.7	4	1
Total			35	4

thereby that a warm layer existed in the lower troposphere. The temperature below the warm layer decreases quickly during the process.

The composite sounding (Fig. 15b) for FZRA in the plain included 18 radiosonde observations (Table 2): 6 from Huaihua, 8 from Changsha, and 4 from Nanchang. It also represented all of the observations from mandatory and significant levels. Dry air was typically capped over the cloud layer while FZRA occurred. The composite hodograph was similar to that for IPE. The cloud top was above the warm layer and the temperature of the cloud top was greater than -10°C . A composite of 17 observations from Guiyang for FZRA in the plateau (Fig. 15c) showed that the cloud top was within the warm layer and the cloud-top temperature was greater than 0°C , which suggested that the mechanism for FZRA in the plateau may be different from that in the plain. The features of the sounding for snowfall were obvious and the composite was not shown. The temperature of the entire air column was less than 0°C , without a warm layer, although an inversion layer existed in the middle troposphere.

The melting process occurs when snow falls into a layer of above-freezing air, melts to form rain or drizzle, and then falls into a layer of subfreezing air to become supercooled rain or drizzle. Both Hanesiak and Stewart (1995) and Zerr (1997) found that incomplete melting of snowflakes in the warm layer was the primary factor in the production of IPE. On the basis of the above analyses, incomplete melting of snowflakes in the warm layer may be the mechanism for IPE formation, and melting processes may be the formation mechanisms for FZRA. The strength and depth of the cold layer near the surface was examined and it was found that the cold layer for IPE is stronger and deeper than that for FZRA.

4. Conceptual model for long-duration freezing precipitation

A conceptual model is proposed to explain the long duration of freezing precipitation over southern China. Shown in Fig. 16a are the synoptic conditions favorable to the invasion of cold air into southern China, in which

a blocking high pressure system in the north branch of the westerlies at 500 hPa can be found, with a trough or low pressure to the east of the blocking high in eastern Mongolia or northeast China. The south branch trough stagnated over Yunnan Province and the northern Indochina peninsula and transported abundant warm and moisture-laden air to southern China. The warm air from the south and the cold air from the north met in southern China and formed the inversion and warm layer in the lower troposphere, which was very favorable for the occurrence of freezing precipitation.

The most important system producing freezing precipitation was a quasi-stationary front (shear line) in the lower troposphere. This front extended in the east–west or northeast–southwest directions in southern China during the freezing precipitation. The moisture converged along the front to condense in the middle troposphere. Freezing precipitation might occur when a warm layer ($>0^{\circ}\text{C}$) was formed. Along the vertical cross section of the front, the precipitation types sequentially from north to south were snow, mixed rain and snow, FZRA or IPE, and rain (Fig. 16b). However, the formation of freezing precipitation was determined by many factors, such as the surface temperature, the dewpoint depression, the wind direction and speed, and the stratification as seen in the sounding profiles. Similar to that over North America (Cortinas et al. 2004), the favorable surface conditions for freezing precipitation were between -1° and -3°C in temperature, between 1° and 3°C for the depression in the dewpoint temperature, and weak northeasterly winds.

The sounding profiles favorable for FZRA or IPE can be determined by the cloud-top temperature, PA (warm area), NA (freezing area), and the ratio of PA and NA (see Fig. 16c for annotation). Bourguin (2000) used PA and NA as predictors to discriminate among the precipitation types. The cloud-top temperature was -5° to -10°C for FZRA, and higher than that for IPE. However, the NA in the FZRA soundings was smaller than that in the IPE soundings.

5. Summary and conclusions

This paper has investigated the multiscale meteorological mechanisms for FZRA and snowstorms in southern China from January to February 2008 that brought record-setting damage dating back to 1950. Based on the synoptic patterns, four stages of this disastrous weather process were identified. The study concentrated on the analysis of synoptic conditions, as well as the surface conditions and sounding profiles favorable for the occurrence of this severe event. The main results can be summarized as follows:

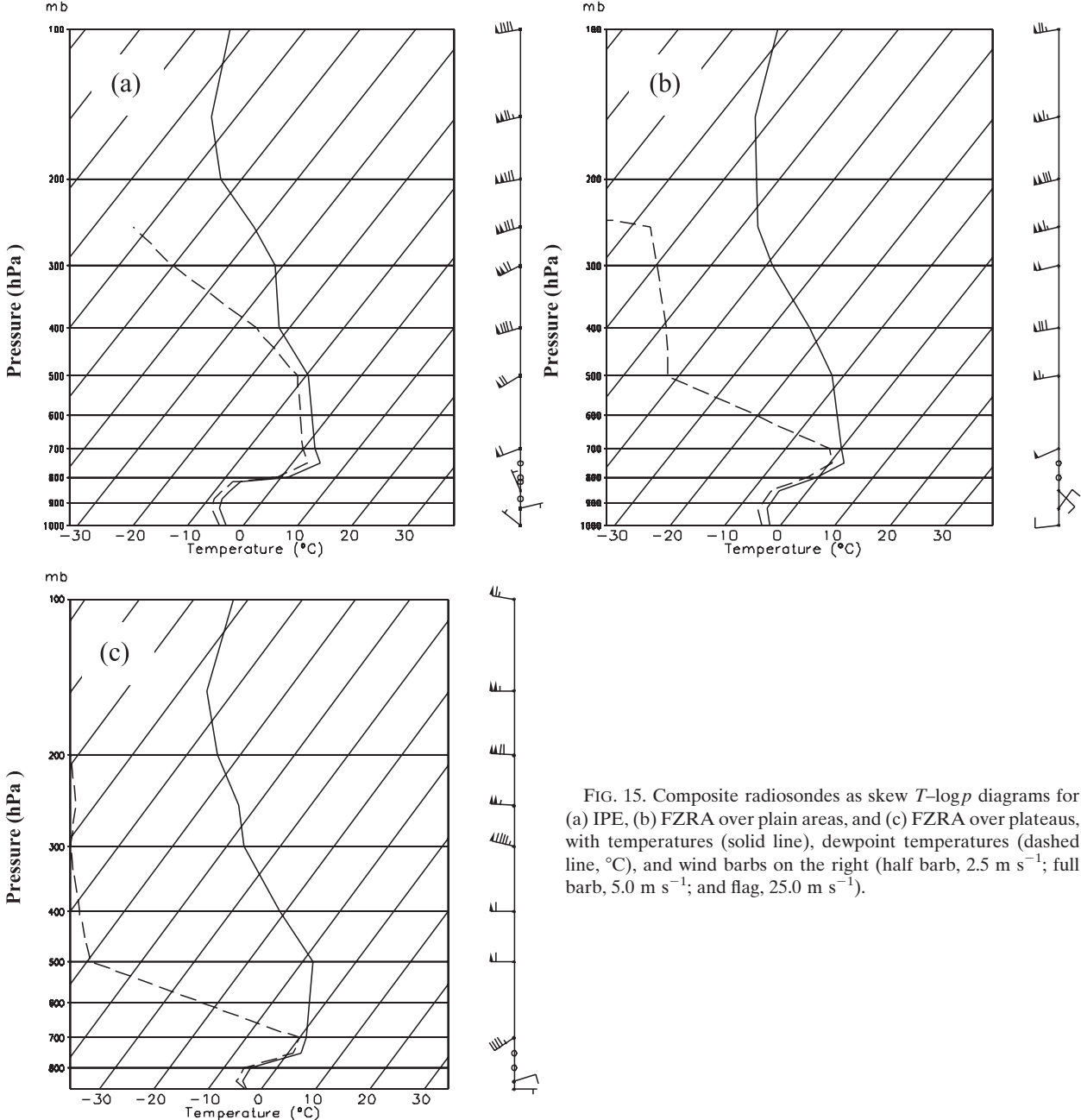


FIG. 15. Composite radiosondes as skew T - $\log p$ diagrams for (a) IPE, (b) FZRA over plain areas, and (c) FZRA over plateaus, with temperatures (solid line), dewpoint temperatures (dashed line, $^{\circ}\text{C}$), and wind barbs on the right (half barb, 2.5 m s^{-1} ; full barb, 5.0 m s^{-1} ; and flag, 25.0 m s^{-1}).

- 1) The significant and long-duration anomaly conditions of the atmospheric circulation during the process were one of the most important reasons for the freezing precipitation and snowstorms. The blocking high pressure in the middle latitudes was located near western Siberia for more than 20 days, which was very favorable for the maintenance of the freezing precipitation. The trough in the south branch of the westerlies also stayed for an extended period. The southwest current ahead of the trough in the south

branch transported warm and moisture-laden air toward southern China. Cold/dry air from the north and warm/moist air from the south converged in southern China, and then an environment favorable for snowfall and FZRA appeared in different areas at different stages. The long duration of the FZRA process was not forecast correctly according to the forecast evaluations, primarily because of the persistent maintenance of a blocking high lasting about 20 days, which could not be exactly predicted in

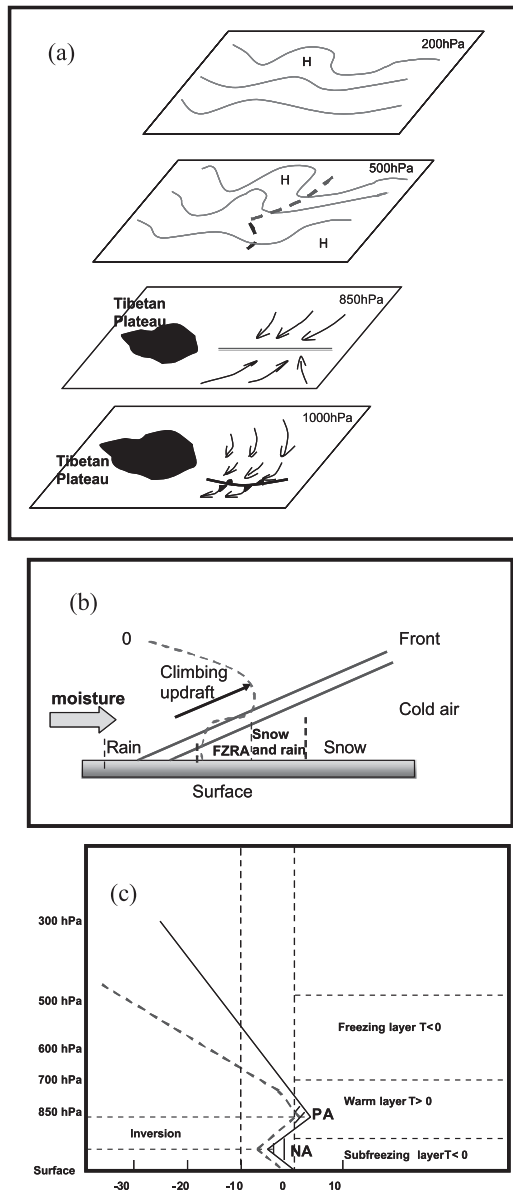


FIG. 16. The multiscale conceptual model for long-duration freezing precipitation events over southern China: (a) synoptic weather pattern, (b) structure of a quasi-stationary front, and (c) stratification conditions for freezing precipitation.

advance. The maintenance mechanism of the long duration of the blocking high pressure is a very difficult topic. Generally, the averaged duration of a blocking high pressure system in the Northern Hemisphere is only about 5 days (Zhao and Mills 1991), which was much less than that in this event.

2) The cloud clusters were very active over the Tibetan Plateau from January to February 2008, propagated eastward, and affected eastern China several times. With the exception of the first stage, the other three

stages (from 18 January to 1 February) exhibited eastward propagation of cloud systems from the Tibetan Plateau.

- 3) It can be seen that the east–west-oriented quasi-stationary front (or shear line) was located over southern China during the long-duration precipitation event. It has been noted that the quasi-stationary front was the most important system producing FZRA and the snowstorms. This front was quite different from the cases in the North America, where warm fronts and extratropical cyclones were reported. This kind of quasi-stationary front has hardly been observed over China during the wintertime prior to 2008. The stronger frontogenesis can be found mainly in the western part of the front than that in the east because the track of cold air moved westward, away from its normal location. A stronger horizontal gradient of the isolines of the pseudo-equivalent potential temperature and the higher temperature of the inversion layer in the western part of the front compared to that of its eastern part can be found. The strongest warm moisture convergence occurred at the front location from the surface to the middle troposphere above, which enhanced the formation, development, and persistence of freezing precipitation in the western part of the front.
- 4) The formation of FZRA was very sensitive to some key influencing factors. The preferred ground surface temperature for FZRA ranged from -1° to -3°C . The warm layer and inversion generally coexisted during the FZRA; at the same time, the formation of FZRA was sensitive to the thickness of both the warm layer and the near-surface frozen layer. However, in some cases, there existed no warm layer in the clouds, for example, in the freezing drizzle processes in Guizhou Province. The freezing drizzle could be frozen directly in mountainous area without a warm layer. It should be noted for forecast purposes that the warm layer must not be necessary for some cases, particularly, in lower-latitude Guizhou Province.
- 5) One possible reason why freezing precipitation events have received so little attention during the last several decades is that they are seldom well documented in China. As demonstrated here, correct forecasts of these severe freezing precipitation events requires clear conceptual models of their structure and evolution. Therefore, a conceptual model was proposed to describe the multiscale weather systems responsible for the long duration of this freezing precipitation event. These systems include the synoptic conditions, details of the quasi-stationary front, and the sounding profiles associated with FZRA. We believe that this conceptual model has the potential

to be used by operational weather forecasters for predicting freezing precipitation events.

In this study, our investigation of freezing precipitation in southern China from January to February 2008 is mainly based on general synoptic analysis methods, while it has been noticed that the complicated interactions between the precipitation and the atmospheric thermodynamics are one of key processes that affect the locations and intensities of various freezing precipitation types. In a future study, we plan to examine this interaction process using numerical modeling experiments.

Acknowledgments. This research was supported by the National Natural Science Foundation of China under Grants 40875021 and 40605016, and the Institute of Heavy Rain, Wuhan, under Grant IHR2007K05.

REFERENCES

- Bernstein, B. C., 2000: Regional and local influences on freezing drizzle, freezing rain, and ice pellet events. *Wea. Forecasting*, **15**, 485–508.
- Bocchieri, J. R., 1980: The objective use of upper air soundings to specify precipitation type. *Mon. Wea. Rev.*, **108**, 596–603.
- Bourguin, P., 2000: A method to determine precipitation types. *Wea. Forecasting*, **15**, 583–592.
- Carrière, J. M., C. Lainard, C. Le Bot, and F. Robart, 2000: A climatological study of surface freezing precipitation in Europe. *Meteor. Appl.*, **7**, 229–238.
- Changnon, S. A., and T. R. Karl, 2003: Temporal and spatial variations of freezing rain in the contiguous United States: 1948–2000. *J. Appl. Meteor.*, **42**, 1302–1315.
- Chen, T. X., G. F. Chen, and X. T. Mu, 1993: The diagnosis and prediction on characteristics of freezing rain at Zhumadian (in Chinese). *Meteor. Monogr.*, **19**, 33–36.
- Coleman, H., and J. Marwitz, 2002: Thermodynamic and kinematic structure of a snowband and freezing rain event during STORM-FEST. *Wea. Forecasting*, **17**, 27–46.
- Cortinas, J. V., B. C. Bernstein, C. C. Robbins, and J. W. Strapp, 2004: An analysis of freezing rain, freezing drizzle, and ice pellets across the United States and Canada: 1976–90. *Wea. Forecasting*, **19**, 377–390.
- Czys, R. R., R. W. Scott, K. C. Tang, R. W. Przybylinski, and M. E. Sabones, 1996: A physically based, nondimensional parameter for discriminating between locations of freezing rain and ice pellets. *Wea. Forecasting*, **11**, 591–597.
- Ding, Y.-H., 1992: Summer monsoon rainfalls in China. *J. Meteor. Soc. Japan*, **70**, 373–396.
- , and T. N. Krishnamurti, 1987: Heat budget of the Siberian high and the winter monsoon. *Mon. Wea. Rev.*, **115**, 2428–2449.
- Forbes, G. S., R. A. Anthes, and D. W. Thomson, 1987: Synoptic and mesoscale aspects of an Appalachian ice storm associated with cold-air damming. *Mon. Wea. Rev.*, **115**, 564–591.
- Hanesiak, J. M., and R. E. Stewart, 1995: The mesoscale and microscale structure of a severe ice pellet storm. *Mon. Wea. Rev.*, **123**, 3144–3162.
- Houston, T. G., and S. A. Changnon, 2007: Freezing rain events: A major weather hazard in the conterminous US. *Nat. Hazards*, **40**, 485–494.
- Huffman, G. J., and G. A. Norman, 1988: The supercooled warm rain process and the specification of freezing precipitation. *Mon. Wea. Rev.*, **116**, 2172–2182.
- Jiang, J. X., and M. Z. Fan, 2002: Convective clouds and mesoscale convective systems over the Tibetan Plateau in summer (in Chinese). *Chinese J. Atmos. Sci.*, **26**, 263–270.
- Keyser, D., and M. A. Shapiro, 1986: A review of the structure and dynamics of upper-level frontal zones. *Mon. Wea. Rev.*, **114**, 452–499.
- Lv, S. H., J. G. Wang, and J. Qiu, 2004: Analysis of freezing rains at Tianjin airport (in Chinese). *Meteor. Sci. Tech.*, **32**, 456–460.
- Rauber, R. M., M. K. Ramamurthy, and A. Tokay, 1994: Synoptic and mesoscale structure of a severe freezing rain event: The St. Valentine's Day ice storm. *Wea. Forecasting*, **9**, 183–208.
- , L. S. Olthoff, M. K. Ramamurthy, and K. E. Kunkel, 2000: The relative importance of warm rain and melting processes in freezing precipitation events. *J. Appl. Meteor.*, **39**, 1185–1195.
- Stewart, R. E., 1985: Precipitation types in winter storms. *Pure Appl. Geophys.*, **123**, 597–609.
- , 1992: Precipitation types in the transition region of winter storms. *Bull. Amer. Meteor. Soc.*, **73**, 287–296.
- , and P. King, 1987: Freezing precipitation in winter storms. *Mon. Wea. Rev.*, **115**, 1270–1280.
- Tao, S. Y., 1980: *Heavy Rainfall in China* (in Chinese). Science Press, 225 pp.
- , and Y. H. Ding, 1981: Observational evidence of the influence of the Qinghai-Xizang (Tibet) Plateau on the occurrence of heavy rain and severe convective storms in China. *Bull. Amer. Meteor. Soc.*, **62**, 23–30.
- , and L. Chen, 1987: A review of recent research on the East Asian summer monsoon in China. *Monsoon Meteorology*, C.-P. Chang and T. N. Krishnamurti, Eds., Oxford University Press, 60–92.
- Yang, X. D., 1999: The diagnosis on a freezing rain at Tiaoxian airport (in Chinese). *Liaoning Meteor. Quart.*, **16**, 11–12.
- Yasunari, T., and T. Miwa, 2006: Convective cloud systems over the Tibetan Plateau and their impact on meso-scale disturbance in the Meiyu/Baiu frontal zone. *J. Meteor. Soc. Japan*, **84**, 783–803.
- Ye, Y., X. L. Du, and X. D. Yan, 2007: The spatial and temporal distribution of freezing rain at Guizhou and its circulations (in Chinese). *J. Guizhou Meteor.*, **31** (6), 11–13.
- Zerr, R. J., 1997: Freezing rain: An observational and theoretical study. *J. Appl. Meteor.*, **36**, 1647–1661.
- Zhang, S. L., S. Y. Tao, Q. Y. Zhang, and J. Wei, 2002: The characteristics of scales in heavy rainfalls with floods along the Yangtze River. *Chin. Sci. Bull.*, **47**, 467–473.
- Zhao, L. N., and Coauthors, 2008: The impact and the disasters of a severe snow and freezing rain over southern China in the early of 2008. (in Chinese). *Climatic Environ. Res.*, **14**, 556–566.
- Zhao, S., and G. A. Mills, 1991: A study of a monsoon depression bringing record rainfall over Australia. Part II: Synoptic-diagnostic description. *Mon. Wea. Rev.*, **119**, 2074–2094.
- , Z. Y. Tao, J. H. Sun, and N. F. Bei, 2004: *Study on Mechanism of Formation and Development of Heavy Rainfalls on Mei-Yu Front in Yangtze River* (in Chinese). China Meteorological Press, 282 pp.